# Handbook of Electrochemical Impedance Spectroscopy. DISTRIBUTED and MIXED IMPEDANCES

**Technical Report** · July 2020

DOI: 10.13140/RG.2.2.14198.01606



**3 authors**, including:

Jean-Paul Diard
BioLogic


Bernard Le Gorrec
UJFG-INPG

# Handbook
# of
# Electrochemical Impedance Spectroscopy

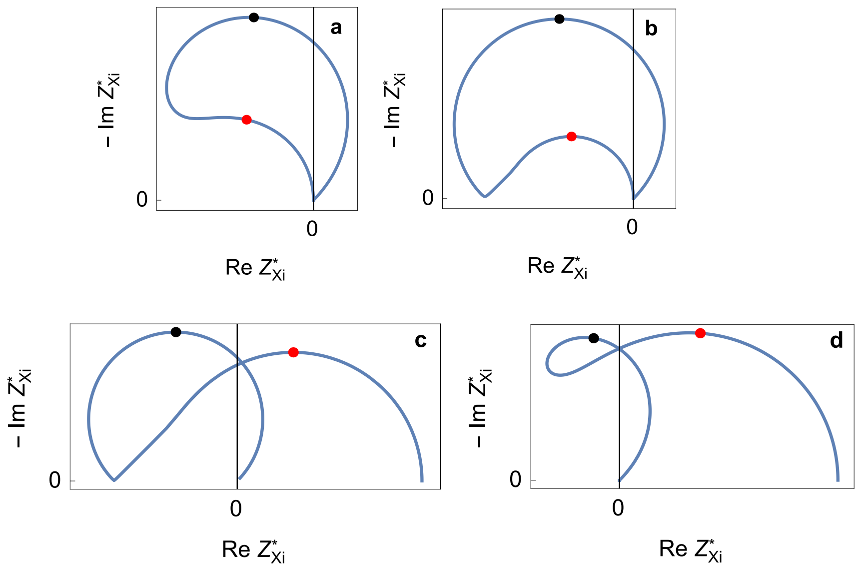


## DISTRIBUTED
## and
## MIXED IMPEDANCES

ER@SE/LEPMI
J.-P. Diard, B. Le Gorrec, C. Montella

July 16, 2020

# Contents

# Chapter 1

# Introduction

## 1.1 Lumped *vs.* distributed systems

### 1.1.1 Lumped systems

The transfer functions of systems modeled by ordinary differential equations, often called lumped-parameter systems, are rational functions (i.e. a ratio of two polynomials in $s$, the Laplace variable) [1, 2].

### 1.1.2 Distributed systems

The transfer functions of distributed parameter systems are irrational functions. The analysis of rational and irrational transfer functions differ in a number of important aspects. The most obvious differences between rational and irrational transfer functions are the poles and zeros. Irrational transfer functions often have infinitely many poles and zeros [2].

### 1.1.3 Mixed lumped-distributed systems

The transfer functions of mixed lumped-distributed systems contain rational and irrational functions in $s$.

## 1.2 Examples in electrochemistry

### 1.2.1 Lumped systems

Faradaic impedance $Z_\mathrm{f}$ and impedance $Z$ of electrochemical adsorption reaction (EAR) are lumped systems [3, 4]. Eq. (1.1) is a rational fraction in $s$ ([1]).

$$Z(s) = \frac{1 + R_\mathrm{ct} C_\mathrm{ads} s}{s\left((C_\mathrm{dl} + C_\mathrm{ads}) + s R_\mathrm{ct} C_\mathrm{dl} C_\mathrm{ads}\right)} \tag{1.1}$$

$$Z(s) = K \frac{1 + \alpha\, s}{s\,(1 + \beta\, s)}, K = \frac{1}{C_\mathrm{dl} + C_\mathrm{ads}},\ \alpha = R_\mathrm{ct} C_\mathrm{ads},\ \beta = \frac{R_\mathrm{ct} C_\mathrm{dl} C_\mathrm{ads}}{C_\mathrm{dl} + C_\mathrm{ads}} \tag{1.2}$$

[1] Replacing a capacitor, for example $C_\mathrm{dl}$, by a CPE [5] transforms a lumped impedance in a distributed impedance. This case is not subsequently envisaged.

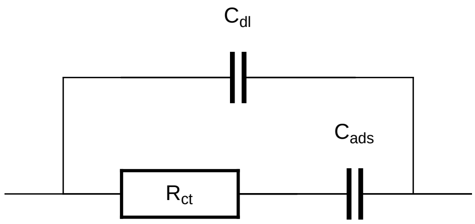


Figure 1.1: Equivalent circuit for electrochemical adsorption reaction (EAR).

### 1.2.2 Distributed systems

The Faradaic impedance of a corroding electrode with mass transfer limitation (Fig 1.2) is a rational fraction in $\sqrt{s}$, i.e. an irrational fraction in $s$.

$$Z_{\mathrm{f}}(s) = \frac{R\,\sigma}{\sigma + R\sqrt{s}} \tag{1.3}$$

$$Z_{\mathrm{f}}(s) = \frac{K}{1+\alpha\sqrt{s}},\ K = R,\ \alpha = \frac{R}{\sigma} \tag{1.4}$$

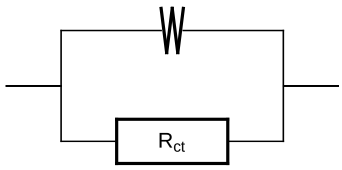


Figure 1.2: Equivalent circuit for a corroding electrode with mass transfer limitation. W: Warburg element for semi-innite linear diffusion [6].

### 1.2.3 Mixed lumped-distributed systems

The impedance of the Randles equivalent circuit [4, 6, 7] (Fig. 1.3) is a mixed lumped and distributed system:

$$Z(s) = \frac{R_{\mathrm{ct}} + R_{\mathrm{d}} \dfrac{\mathrm{th}\sqrt{\tau_{\mathrm{d}} s}}{\sqrt{\tau_{\mathrm{d}} s}}}{1 + R_{\mathrm{ct}} C_{\mathrm{dl}}\, s + C_{\mathrm{dl}}\, s\, R_{\mathrm{d}} \dfrac{\mathrm{th}\sqrt{\tau_{\mathrm{d}} s}}{\sqrt{\tau_{\mathrm{d}} s}}} \tag{1.5}$$

$$Z(s) = K \frac{1 + \alpha \dfrac{\mathrm{th}\sqrt{\tau_{\mathrm{d}} s}}{\sqrt{\tau_{\mathrm{d}} s}}}{1 + \beta\, s + \gamma\, s\, \dfrac{\mathrm{th}\sqrt{\tau_{\mathrm{d}} s}}{\sqrt{\tau_{\mathrm{d}} s}}},\ K = R_{\mathrm{ct}}, \alpha = \frac{R_{\mathrm{d}}}{R_{\mathrm{ct}}}, \beta = R_{\mathrm{ct}} C_{\mathrm{dl}}\, \gamma = C_{\mathrm{dl}} R_{\mathrm{d}} \tag{1.6}$$

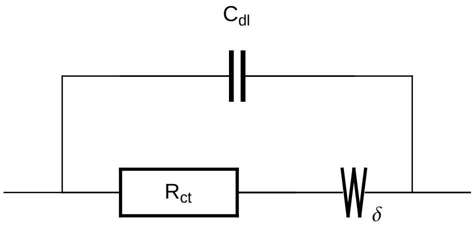


Figure 1.3: Randles equivalent circuit for a redox reactions studied on a rotating disk electrode. $W_\delta$: bounded diffusion impedance [6].

# Chapter 2

# Impedance containing $\dfrac{\mathbf{th}\sqrt{S}}{\sqrt{S}}$

## 2.1 $\dfrac{\mathbf{th}\sqrt{S}}{\sqrt{S}}$

### 2.1.1 Electrochemical reaction

Redox reaction [4, 8, 9]:

$$\mathrm{O} + \mathrm{e} \leftrightarrow \mathrm{R}$$

studied on a rotating disk electrode with mass transfer limitation.

### 2.1.2 Electrochemical impedance

$$Z_{\mathrm{W}_\delta}(s) = R_\mathrm{d}\,\frac{\mathrm{th}\sqrt{\tau\,s}}{\sqrt{\tau\,s}} \ \ ({}^1) \tag{2.1}$$

### 2.1.3 Reduced impedance

$$Z_{\mathrm{W}_\delta}(s) = R_\mathrm{d}\,\frac{\mathrm{th}\sqrt{\tau\,s}}{\sqrt{\tau\,s}} \Rightarrow Z(S) = \frac{Z_{\mathrm{W}_\delta}(s)}{R_\mathrm{d}} = \frac{\mathrm{th}\sqrt{S}}{\sqrt{S}},\ S = \tau\,s = \Sigma + \mathrm{i}\,u \tag{2.2}$$

### 2.1.4 Pole-zero map

Infinite product expansion [12–16]:

$$\frac{\mathrm{th}\sqrt{S}}{\sqrt{S}} = \frac{1}{1+\dfrac{4\,S}{\pi^2}}\prod_{k=1}^{\infty}\frac{1+\dfrac{S}{(k\,\pi)^2}}{1+\dfrac{4\,S}{((2\,k+1)\,\pi)^2}} = P_\infty \tag{2.3}$$

Thanks to Eq. (2.3)

[1] This expression could be replaced by a more accurate one [10, 11]. This case is not subsequently envisaged.

- infinity of interlaced real poles and zeros (Fig. 2.1).

$$s_{\mathrm{p}} = -\frac{1}{4}((2k+1)\,\pi)^2,\ k = 1 \cdots \infty \tag{2.4}$$

$$s_{\mathrm{Z}} = -(k\,\pi)^2,\ k = 1 \cdots \infty \tag{2.5}$$

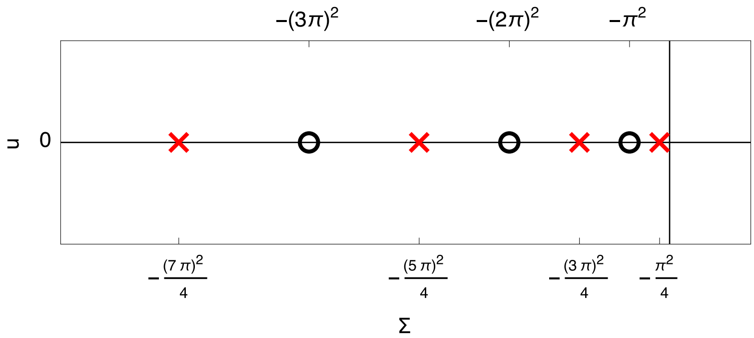


Figure 2.1: Pole-zero map of $\frac{\mathrm{th}\sqrt{S}}{\sqrt{S}}$.

### 2.1.5 Graph of the reduced impedance

3D plot of the modulus (Fig. 2.2).

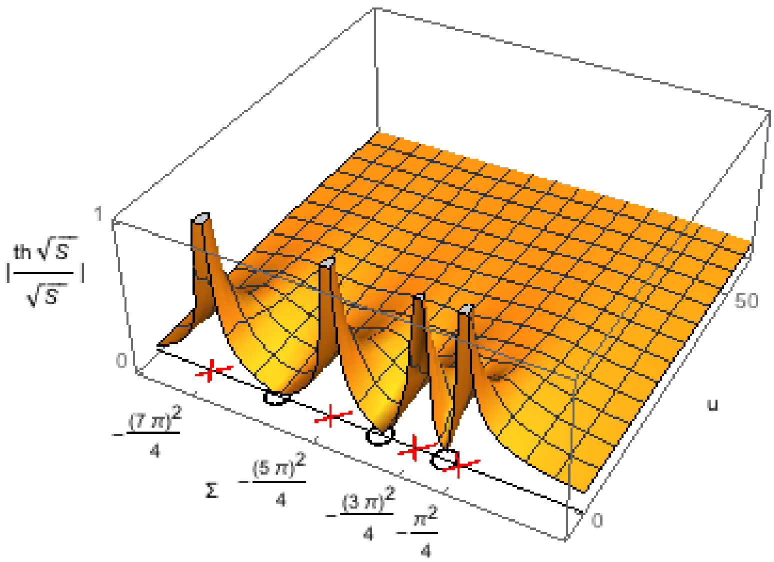


Figure 2.2: 3D plot of the modulus of $\frac{\mathrm{th}\sqrt{S}}{\sqrt{S}}$.

## 2.2 $\dfrac{\frac{\mathbf{th}\sqrt{S}}{\sqrt{S}}}{1+\alpha\frac{\mathbf{th}\sqrt{S}}{\sqrt{S}}}$

### 2.2.1 Electrochemical reaction

Corroding electrode with mass transfert limitation:

$$\mathrm{M} \rightarrow \mathrm{M}^{n+} + n\ \mathrm{e}^-$$
$$\mathrm{O_2} + 4\ \mathrm{e}^- + 4\ \mathrm{H}^+ \rightarrow 2\ \mathrm{H_2O}$$

### 2.2.2 Reduced Faradaic impedance

$$Z(S) = \frac{\frac{\mathrm{th}\sqrt{S}}{\sqrt{S}}}{1+\alpha\frac{\mathrm{th}\sqrt{S}}{\sqrt{S}}},\ u_{c1} = 2.54, u_{c2} = \alpha^2 \tag{2.6}$$

### 2.2.3 Nyquist diagrams

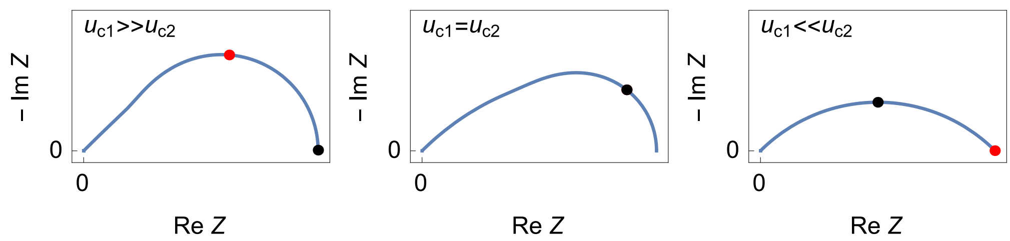


Figure 2.3: Nyquist diagrams calculated from Eq. (2.6). Red dots : $u_{c1} = 2.54$, black dots : $u_{c2} = \alpha^2$.

- $u_{c1} \gg u_{c2}, 2.54 \gg \alpha^2\ \Rightarrow$ quarter of a lemniscate,
- $u_{c1} \ll u_{c2}, 2.54 \ll \alpha^2\ \Rightarrow$ quarter of a circle (see Annex A.2).

## 2.3 $\dfrac{\left(1+\alpha\,\dfrac{\mathbf{th}\sqrt{S}}{\sqrt{S}}\right)\,\dfrac{\mathbf{th}\sqrt{S}}{\sqrt{S}}}{1+\beta\,\dfrac{\mathbf{th}\sqrt{S}}{\sqrt{S}}}$

### 2.3.1 Electrochemical reaction

EE reaction [17]:

$$\begin{array}{l} \mathrm{R} \leftrightarrow \mathrm{X} + \mathrm{e} \\ \mathrm{X} \leftrightarrow \mathrm{O} + \mathrm{e} \end{array}$$

studied on a rotating disk electrode with $D_{\mathrm{R}} = D_{\mathrm{X}} = D_{\mathrm{O}}$.

### 2.3.2 Reduced concentration impedance

Concentration impedances of soluble species:

$$Z_{\mathrm{X}_i}(S) = \frac{\left(1+\alpha\,\dfrac{\mathrm{th}\sqrt{S}}{\sqrt{S}}\right)\,\dfrac{\mathrm{th}\sqrt{S}}{\sqrt{S}}}{1+\beta\,\dfrac{\mathrm{th}\sqrt{S}}{\sqrt{S}}},\ \alpha,\beta \gtrless 0 \tag{2.7}$$

### 2.3.3 Nyquist diagrams

Figs. 2.4, 2.5 and 2.6.

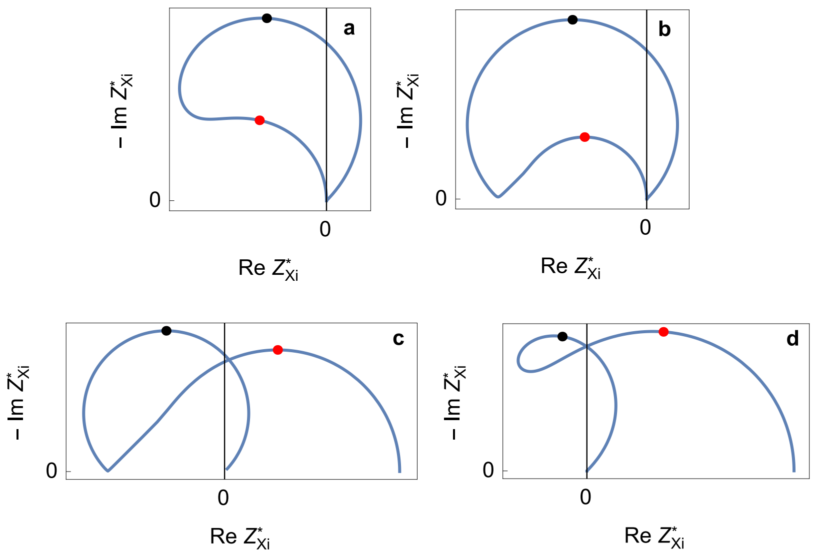


Figure 2.4: Some amazing Nyquist diagrams calculated from Eq. (2.7), $\alpha = -1$, $\beta = -10$ (left), $\beta = -10^4$ (right). Red dots : $u_{c1} = 2.54$, black dots : $u_{c2} = \beta^2$. a: $\alpha = -1$, $\beta = -10$, b: $\alpha = -1$, $\beta = -10^{-4}$, c: $\alpha = -2.5$, $\beta = -10^{-5}$, d: $\alpha = -2.5$, $\beta = -10$ (Hokusai's great wave).

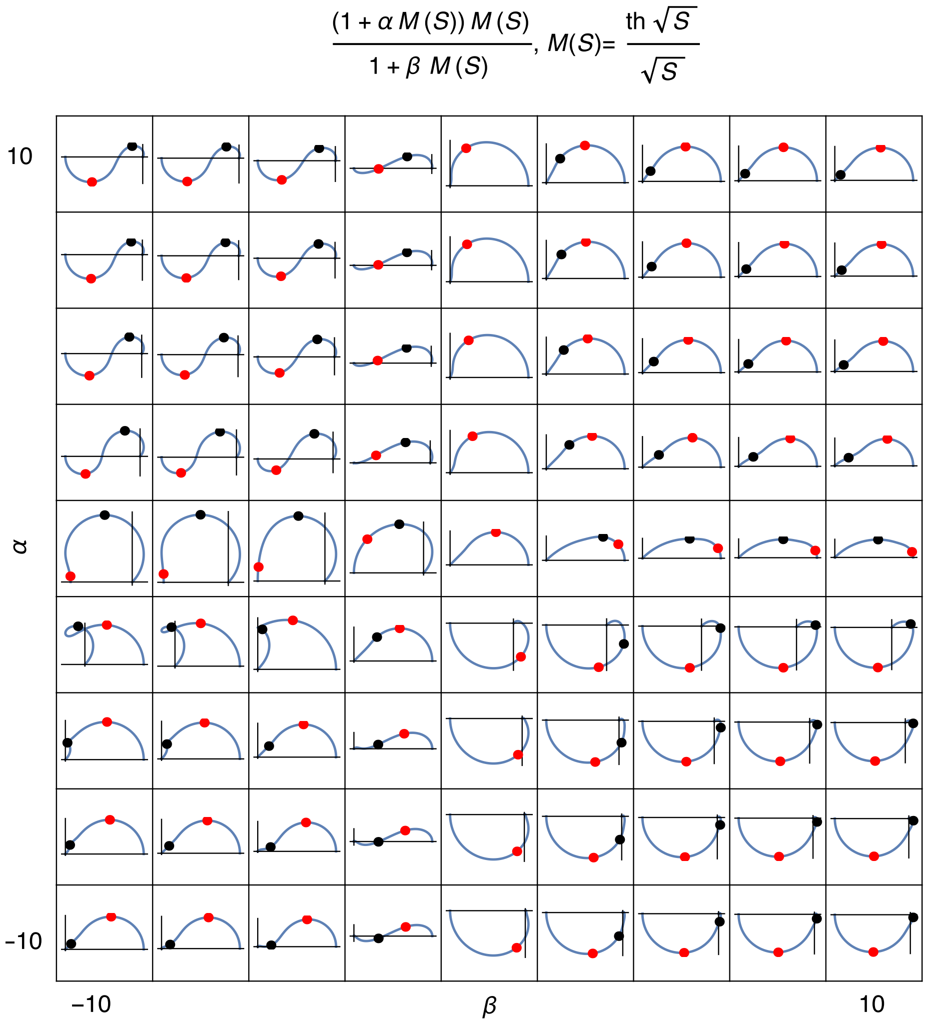


Figure 2.5: Array of impedance diagrams calculated from Eq. (2.7). Red dots : $u_{c1} = 2.54$, black dots : $u_{c2} = \beta^2$.

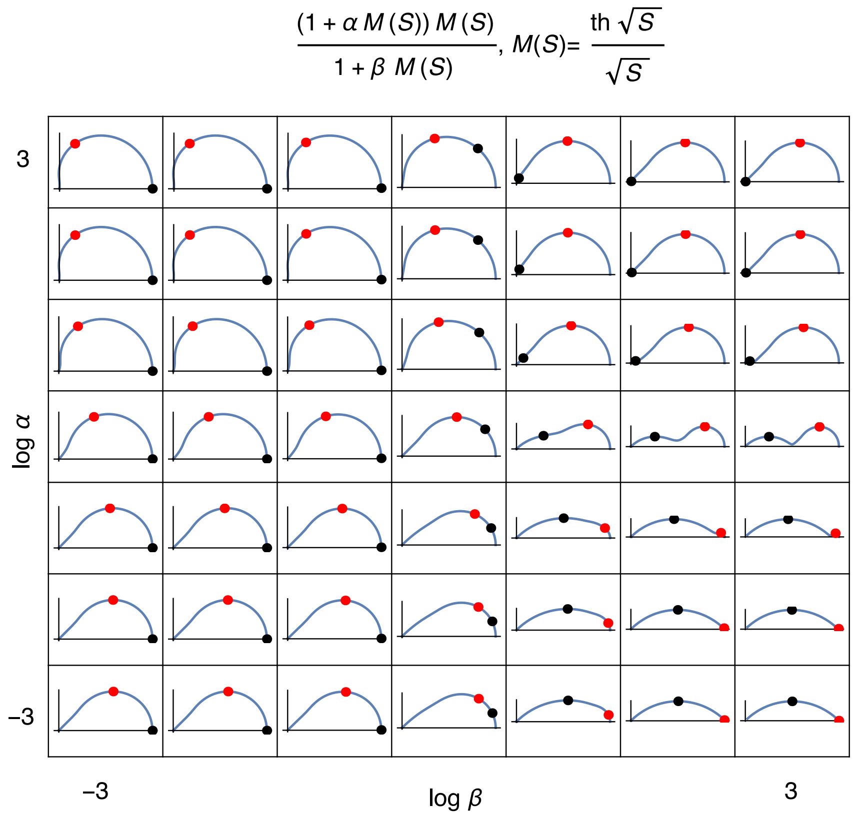


Figure 2.6: Array of impedance diagrams calculated from Eq. (2.7). Red dots : $u_{c1} = 2.54$.

# Chapter 3

# Impedance containing lumped and distributed elements

## 3.1 $\dfrac{\frac{\mathbf{th}\sqrt{S}}{\sqrt{S}}}{1+\alpha\,S}$

$$Z(S) = \frac{\frac{\mathrm{th}\sqrt{S}}{\sqrt{S}}}{1+\alpha\,S} \tag{3.1}$$

Characteristic frequencies:

- $u_{c1} = 2.54$
- $u_{c2} = 1/\alpha$

### 3.1.1 Pole-zero map

- Same zeros as $\dfrac{\mathrm{th}\sqrt{S}}{\sqrt{S}}$
- Same poles as $\dfrac{\mathrm{th}\sqrt{S}}{\sqrt{S}}$ plus one real pole $(-\dfrac{1}{\alpha})$ (Figs. 3.4-3.1).

### 3.1.2 Nyquist diagrams

Figs. 3.4-3.1.

- $u_{c1} \ll u_{c2} \Rightarrow Z(S) \approx \dfrac{\mathrm{th}\sqrt{S}}{\sqrt{S}}$
- $u_{c1} \gg u_{c2} \Rightarrow Z(S) \approx \dfrac{1}{1+\alpha\,S}$

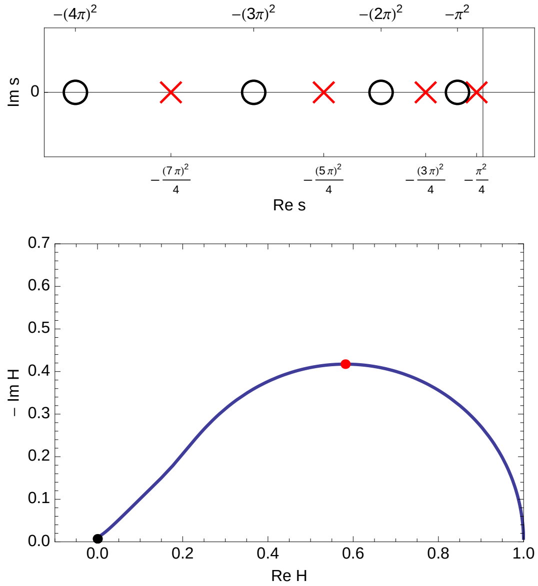


Figure 3.1: Pole-zero map and Nyquist diagram of $\dfrac{1}{1+\alpha\, S}\,\dfrac{\operatorname{th}\sqrt{S}}{\sqrt{S}}$. $\alpha = 10^{-4}$. Red dot: $u_{c1} = 2.54$, black dot: $u_{c2} = 1/\alpha$.

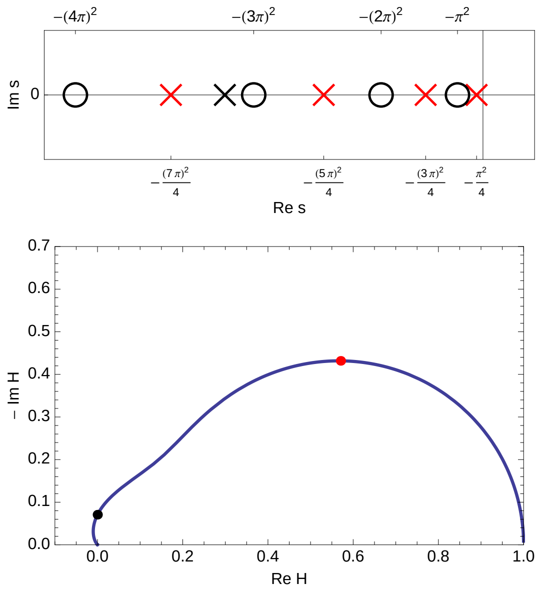


Figure 3.2: Pole-zero map and Nyquist diagram of $\dfrac{1}{1+\alpha\, S}\,\dfrac{\operatorname{th}\sqrt{S}}{\sqrt{S}}$. $\alpha = 10^{-2}$. Red dot: $u_{c1} = 2.54$, black dot: $u_{c2} = 1/\alpha$.

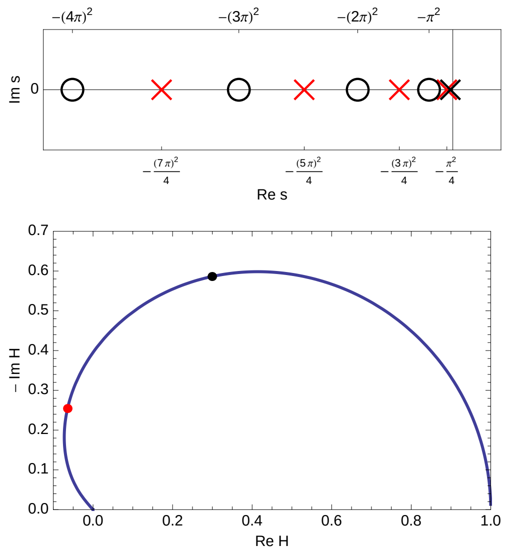


Figure 3.3: Pole-zero map and Nyquist diagram of $\dfrac{1}{1+\alpha\,S}\,\dfrac{\mathrm{th}\sqrt{S}}{\sqrt{S}}$. $\alpha = 1$ $(-\dfrac{1}{\alpha} > -\dfrac{\pi^2}{4})$. Red dot: $u_{c1} = 2.54$, black dot: $u_{c2} = 1/\alpha$.

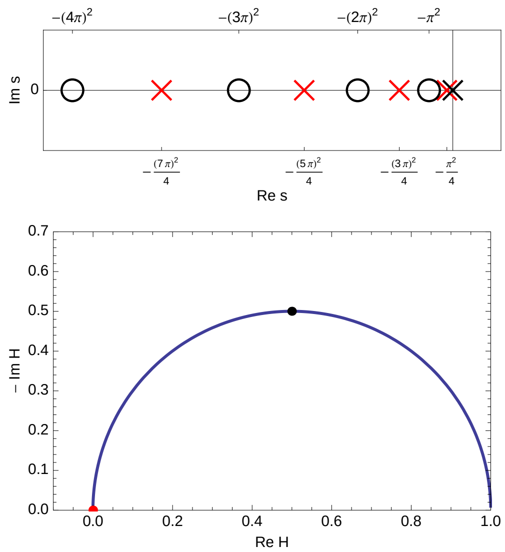


Figure 3.4: Pole-zero map and Nyquist diagram of $\dfrac{1}{1+\alpha\,s}\,\dfrac{\mathrm{th}\sqrt{S}}{\sqrt{S}}$. $\alpha = 10^3$ $(-\dfrac{1}{\alpha} > -\dfrac{\pi^2}{4})$. Red dot: $u_{c1} = 2.54$, black dot: $u_{c2} = 1/\alpha$.

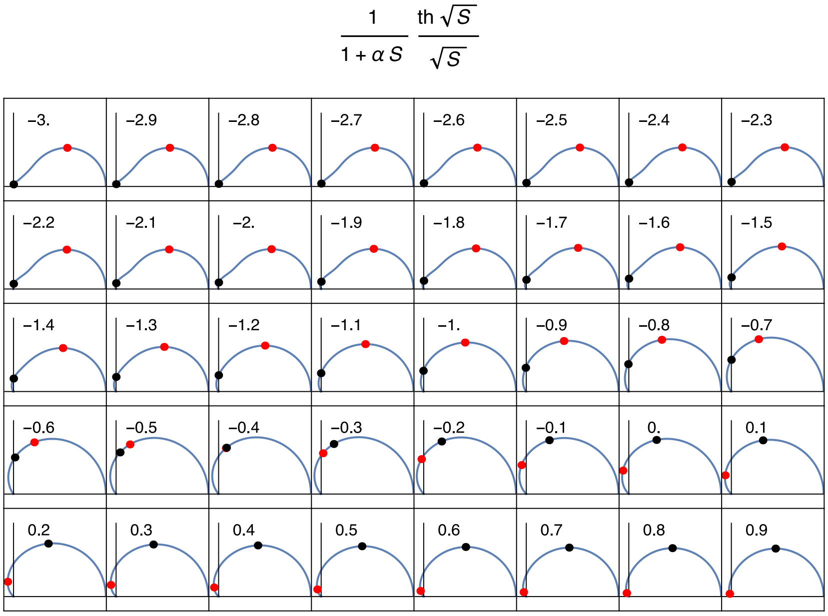


Figure 3.5: Change of Nyquist diagram of $\dfrac{1}{1+\alpha\, S}\,\dfrac{\text{th}\sqrt{S}}{\sqrt{S}}$ with increasing value of $\alpha$ from $10^{-3}$ to $10^{0.9}$. Decimal logarithm of $\alpha$ reported on the Nyquist diagrams. Red dots: $u_{\text{c}1} = 2.54$, black dots: $u_{\text{c}2} = 1/\alpha$.

## 3.2 $\frac{1+\alpha\frac{\mathrm{th}\sqrt{S}}{\sqrt{S}}}{1+\beta S}$

### 3.2.1 Electrochemical reaction: Volmer-Heyrovský (V-H)

Electrochemical reaction: Volmer-Heyrovský (V-H) [4, 8]

$$A^+ + s + e^- \rightarrow A{,}s$$
$$A^+ + A{,}s + e^- \rightarrow A_2 + s$$

### 3.2.2 Reduced concentration impedance of adsorbed species

$$Z_\theta^*(S) = \frac{1+\alpha\frac{\mathrm{th}\sqrt{S}}{\sqrt{S}}}{1+\beta S} = \frac{1}{1+\beta S} + \frac{\alpha\frac{\mathrm{th}\sqrt{S}}{\sqrt{S}}}{1+\beta S} \tag{3.2}$$

$$\alpha \rightarrow \infty \Rightarrow Z_\theta^*(S) \approx \alpha\frac{\mathrm{th}\sqrt{S}}{\sqrt{S}} \Rightarrow u_{c1} = 2.54 \tag{3.3}$$

$$\alpha \rightarrow 0 \Rightarrow Z_\theta^*(S) \approx \frac{1}{1+\beta\,\mathrm{i}\,u} \Rightarrow u_{c2} = \frac{1}{\beta} \tag{3.4}$$

### 3.2.3 Nyquist diagrams

Figs. 3.6 and 3.7.

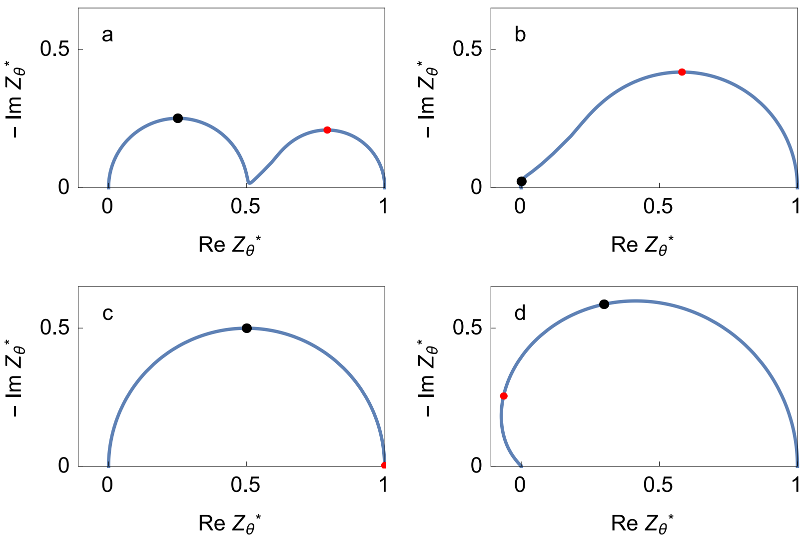


Figure 3.6: Impedance diagrams calculated from Eq. (3.2)). a : $\alpha = 1$, $\beta = 10^{-5}$, b : $\alpha = 10^3$, $\beta = 10^{-3}$, c : $\alpha = 10^{-3}$, $\beta = 10^{-3}$, d : $\alpha = 10^3$, $\beta = 1$. Characteristic dimensionless frequencies: red dots : $u_{c1} = 2.54$, black dots : $u_{c2} = 1/\beta$.

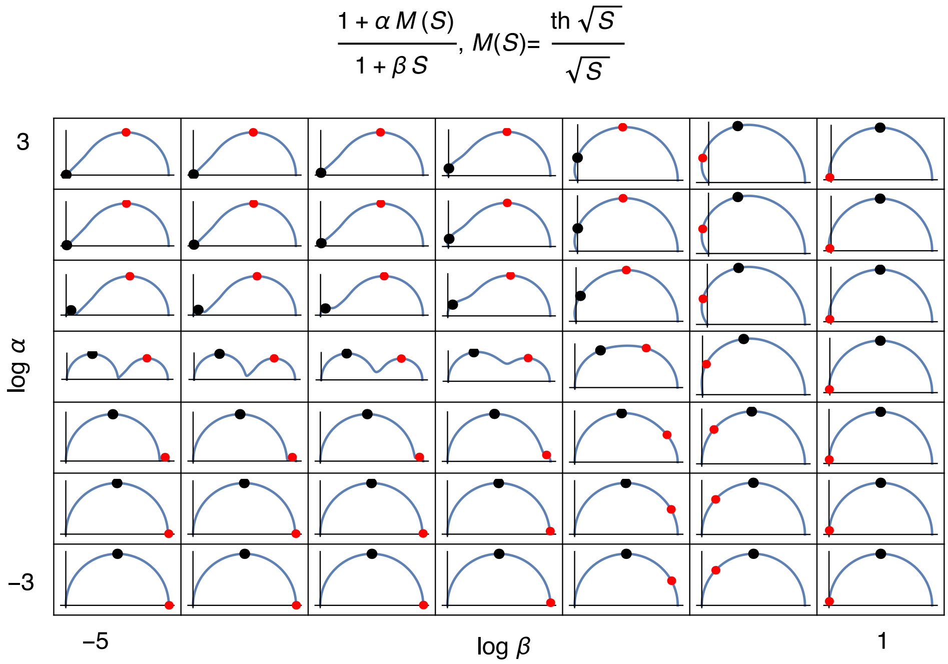


Figure 3.7: Array of impedance diagrams calculated from Eq. (3.2). Impedance diagrams are made of one or two arcs. Characteristic dimensionless frequencies: red dots : $u_{c1} = 2.54$, black dots : $u_{c2} = 1/\beta$.

## 3.3 $\frac{1}{1+\alpha\,S+\beta\,S\,\frac{\mathbf{th}\sqrt{S}}{\sqrt{S}}}$

### 3.3.1 Electrochemical reaction: catalytic copper deposition

$$\mathrm{Cu^{2+}+Cl^{-} + s + e^{-} \rightarrow CuCl,s}$$
$$\mathrm{CuCl,s + e^{-} \rightarrow Cu + Cl^{-} + s}$$

Hypotheses: no mass transfer limitation for $\mathrm{Cu^{2+}}$, $(Cu^{2+}(0,t) \approx Cu^{2+})$, kinetic irreversibility of the two steps [18, 19].

### 3.3.2 Reduced concentration impedance of adsorbed species

$$Z(S) = \frac{1}{1+\alpha\,S+\beta\,S\,\frac{\mathrm{th}\sqrt{S}}{\sqrt{S}}} \tag{3.5}$$

- Poles and zeros of $Z^*(S)$ are real and interlaced.
- Zeros of $Z(S)$ are the poles of $\frac{\mathrm{th}\sqrt{S}}{\sqrt{S}}$: $-\frac{1}{4}((2k+1)\,\pi)^2,\ k = 1\cdots\infty$.
- Characteristic dimensionless frequencies: $u_{\mathrm{c1}} = 2.54$, $u_{\mathrm{c2}} = 1/\alpha$, $u_{\mathrm{c3}} = 1/\beta$

### 3.3.3 Nyquist diagrams

Figs. 3.8 and 3.9.

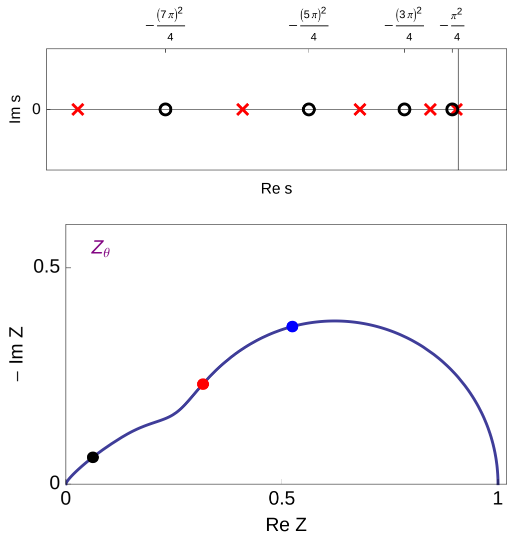


Figure 3.8: Pole-zero map and impedance diagrams calculated from Eq. (3.5). $\alpha = 10^{-2}$, $\beta = 1$, red dot : $u_{c1} = 2.54$, black dot: $u_{c2} = 1/\alpha$, blue dot: $u_{c3} = 1/\beta$.

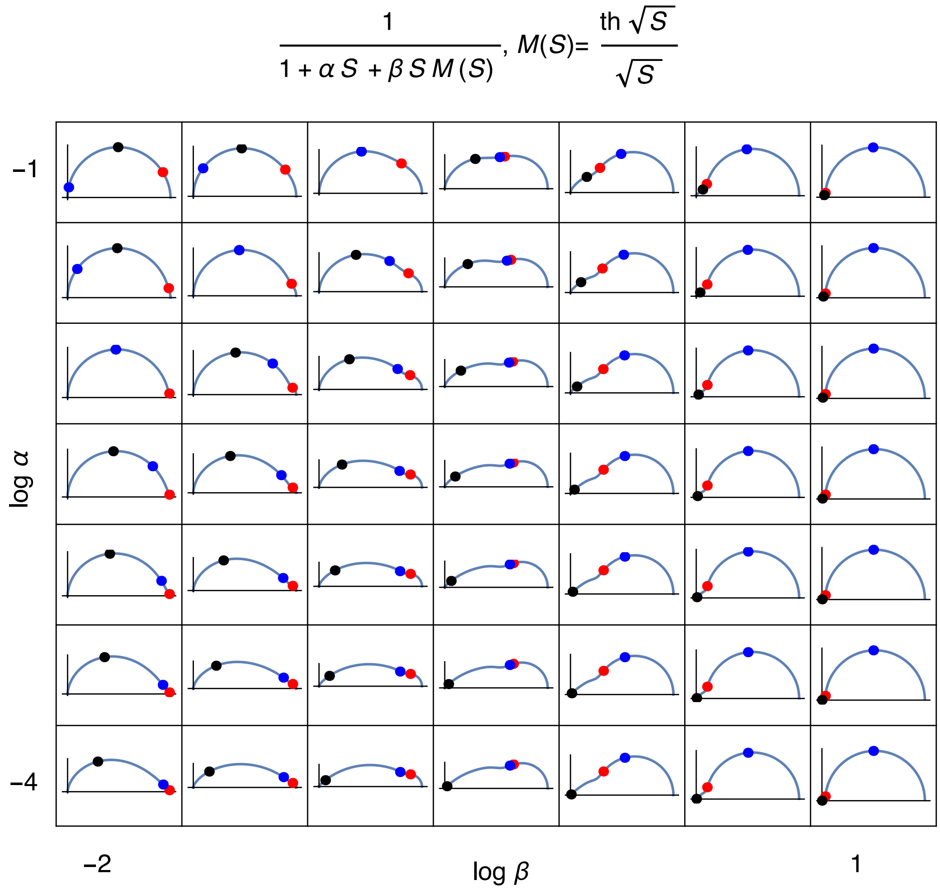


Figure 3.9: Graphics array representation of the impedance diagram, calculated form Eq. (3.5) and plotted using the Nyquist representation (orthonormal scales) for catalytic copper deposition. Characteristic dimensionless frequencies: red dots : $u_{c1} = 2.54$, black dots: $u_{c2} = 1/\alpha$, blue dots: $u_{c3} = 1/\beta$.

## 3.4 $\dfrac{S\,\frac{\mathrm{th}\sqrt{S}}{\sqrt{S}}}{1+\alpha\,S+\beta\,S\,\frac{\mathrm{th}\sqrt{S}}{\sqrt{S}}}$

### 3.4.1 Electrochemical reaction: catalytic copper deposition

$$\mathrm{Cu^{2+} + Cl^- + s + e^- \rightarrow CuCl{,}s}$$
$$\mathrm{CuCl{,}s + e^- \rightarrow Cu + Cl^- + s}$$

Hypotheses: no mass transfer limitation for $Cu^{2+}$, ($Cu^{2+}(0,t) \approx Cu^{2+}$), kinetic irreversibility of the two steps [19].

### 3.4.2 Reduced concentration impedance of soluble species $Cl^-$

$$Z(S) = \frac{S\,\dfrac{\mathrm{th}\sqrt{S}}{\sqrt{S}}}{1+\alpha\,S+\beta\,S\,\dfrac{\mathrm{th}\sqrt{S}}{\sqrt{S}}} \tag{3.6}$$

### 3.4.3 Nyquist diagrams

- Poles and zeros of $Z(S)$ are real.
- Zeros of $Z(S)$ are the zeros of $\dfrac{\mathrm{th}\sqrt{S}}{\sqrt{S}}$ ($S_{\mathrm{Z}} = -(k\,\pi)^2,\ k = 1\cdots\infty$) plus one zero at the origine of the complex plane (derivator).
- Characteristic dimensionless frequencies: $u_{\mathrm{c1}} = 2.54$, $u_{\mathrm{c2}} = 1/\alpha$, $u_{\mathrm{c3}} = 1/\beta$, $u_{\mathrm{c4}} = (\beta/\alpha)^2$.

Fig. 3.10.

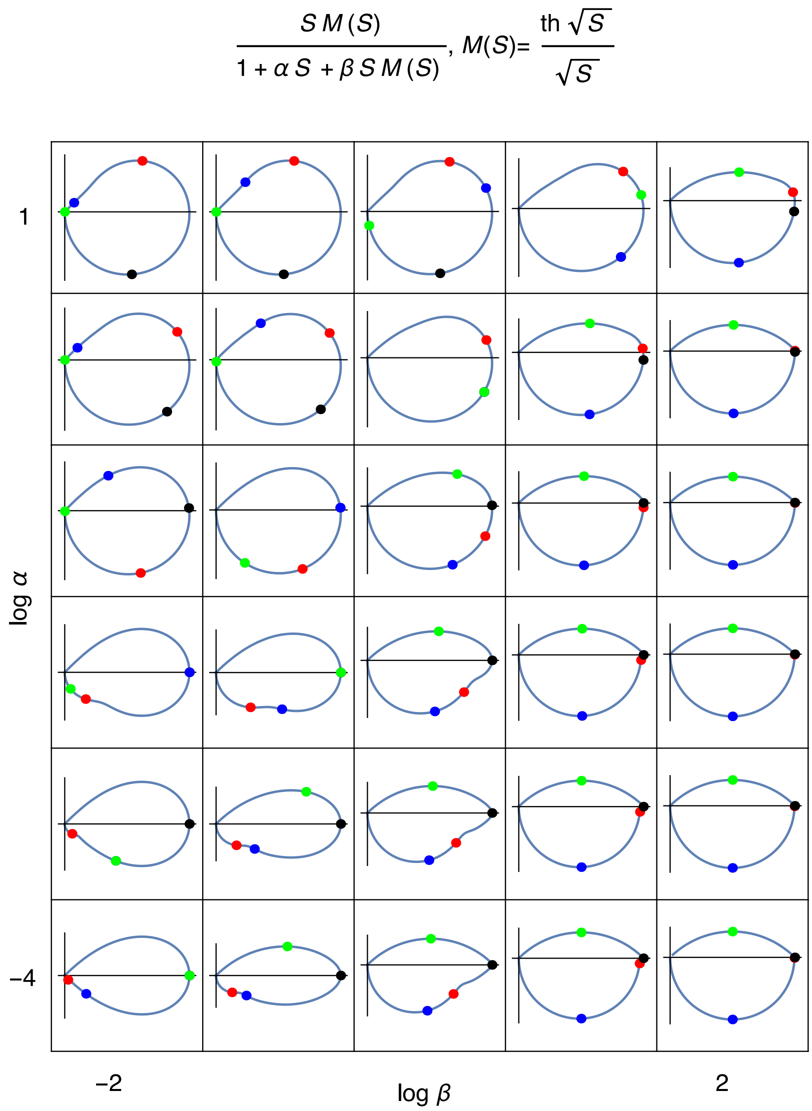


Figure 3.10: Graphics array representation of the reduced impedance diagram calculated from Eq. (3.6) and plotted using the Nyquist complex plane representation (orthonormal scales) for catalytic copper deposition. Characteristic dimensionless frequencies: red dots : $u_{c1} = 2.54$, black dots: $u_{c2} = 1/\alpha$, blue dots: $u_{c3} = 1/\beta$, green dots: $u_{c4} = (\beta/\alpha)^2$.

## 3.5 $\dfrac{1+\alpha\,\frac{\mathrm{th}\sqrt{S}}{\sqrt{S}}}{1+\beta\,S+\gamma\,S\,\frac{\mathrm{th}\sqrt{S}}{\sqrt{S}}}$

### 3.5.1 Electrochemical reaction: E-EAR reaction [20]

$$\mathrm{R + s \rightarrow O + s + n_1\ e}$$
$$\mathrm{A^- + s \leftrightarrow A{,}s + n_2\ e^-}$$

### 3.5.2 Reduced concentration impedance of adsorbed species

$$Z(S) = \frac{1+\alpha\,\dfrac{\mathrm{th}\sqrt{S}}{\sqrt{S}}}{1+\beta\,S+\gamma\,S\,\dfrac{\mathrm{th}\sqrt{S}}{\sqrt{S}}},\ \alpha,\ \beta,\ \gamma \gtrless 0 \tag{3.7}$$

### 3.5.3 Nyquist diagrams

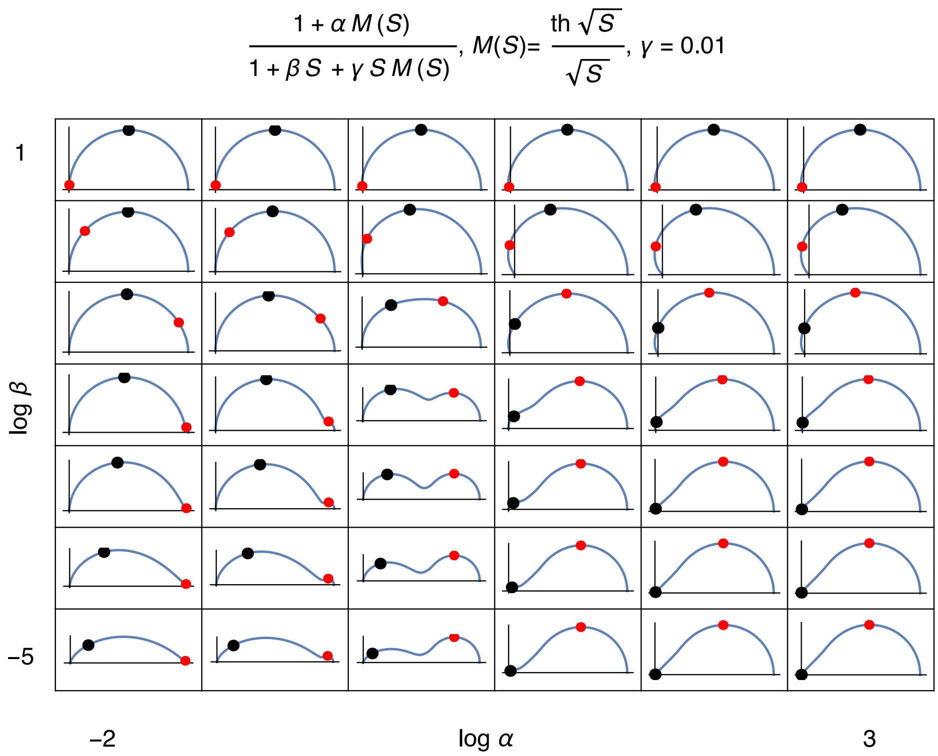


Figure 3.11: Graphics array representation of the Nyquist diagram for the impedance calculated from Eq. (3.7) and plotted using the Nyquist representation (orthonormal scales). Characteristic dimensionless angular frequencies: red dots: $u_{c1} = 2.54$, black dots: $u_{c2} = 1/\beta_1$. $\gamma = 10^{-2}$.

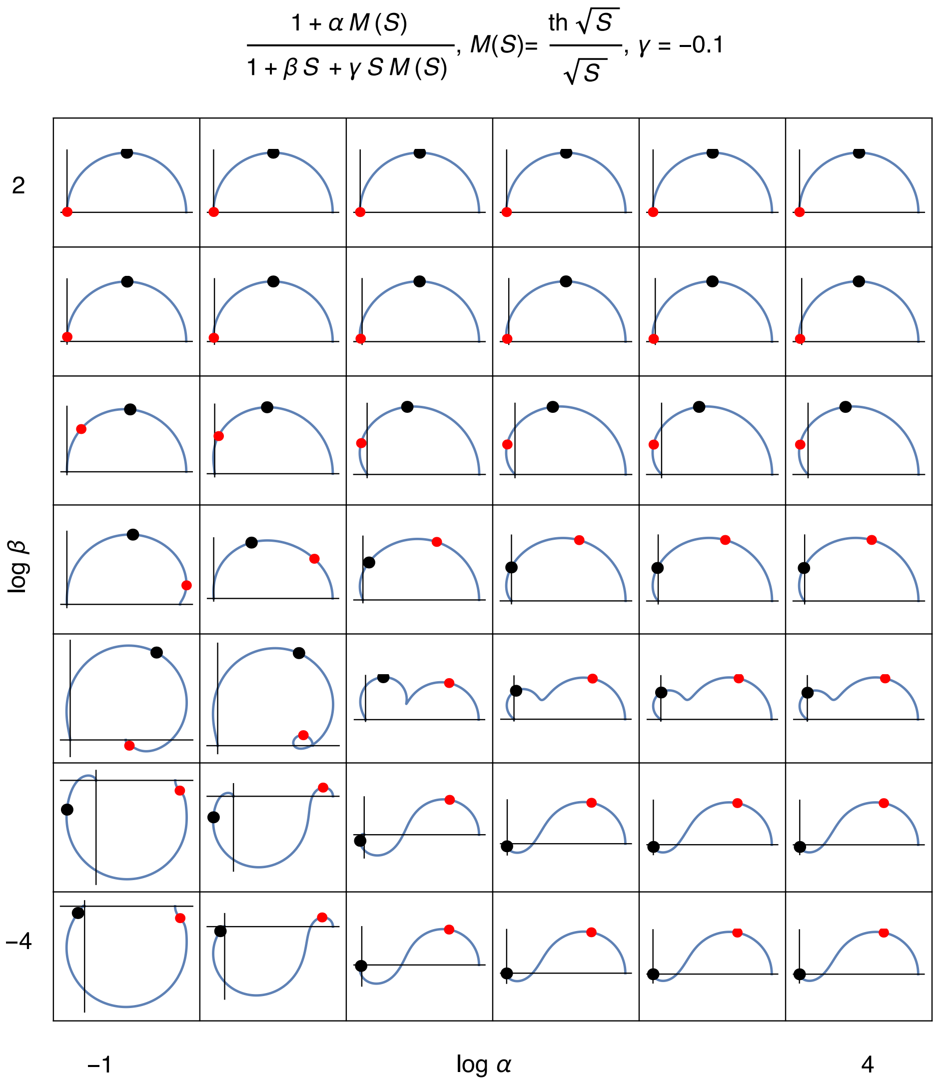


Figure 3.12: Graphics array representation of the Nyquist diagram for the impedance calculated from Eq. (3.7) and plotted using the Nyquist representation (orthonormal scales). Characteristic dimensionless angular frequencies: red dots: $u_{c1} = 2.54$, black dots: $u_{c2} = 1/\beta_1$. $\gamma = -10^{-1}$.

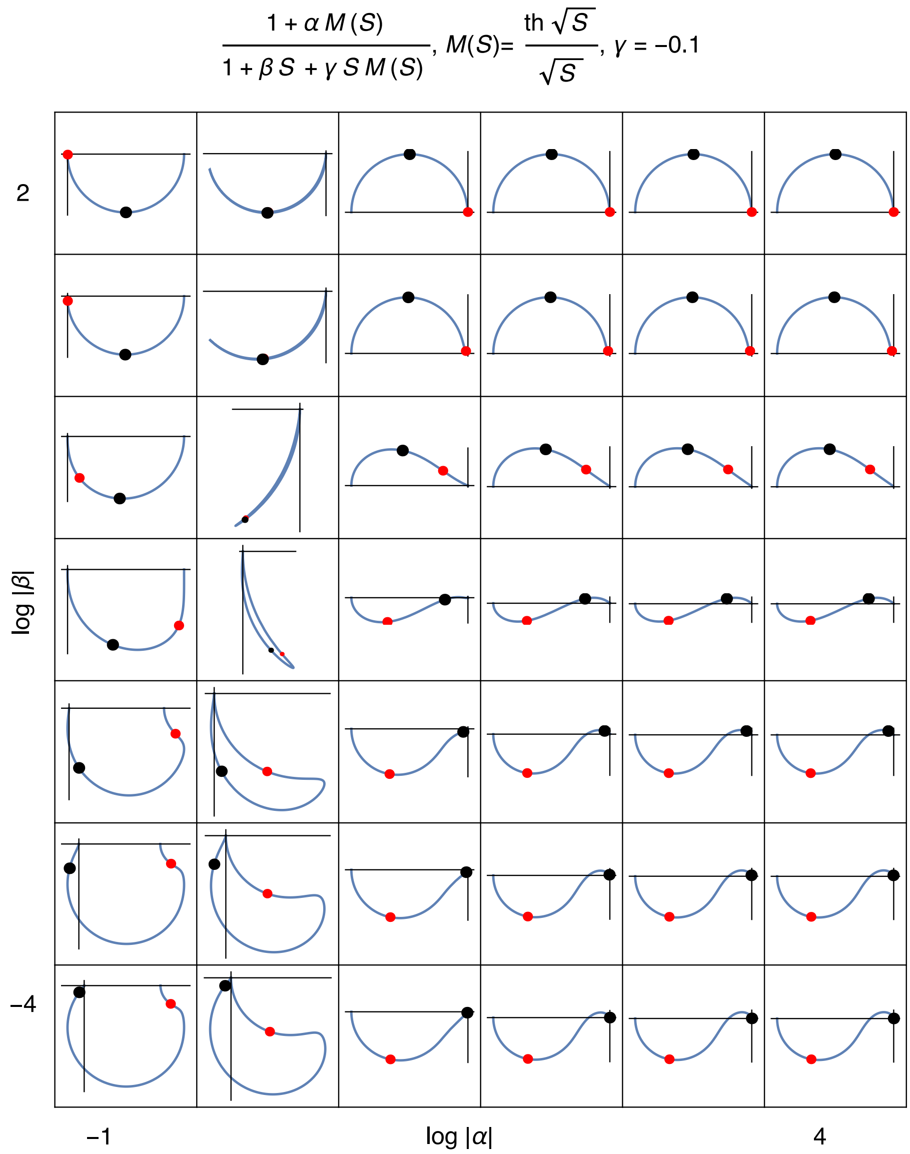


Figure 3.13: Graphics array representation of the Nyquist diagram for the impedance calculated from Eq. 3.7 and plotted using the Nyquist representation (orthonormal scales). $\alpha$, $\beta$, $\gamma < 0$. Characteristic dimensionless angular frequencies: red dots: $u_{c1} = 2.54$, black dots: $u_{c2} = 1/|\beta_1|$. $\alpha, \beta, \gamma < 0$, $\gamma = -10^{-1}$.

## 3.6 $\dfrac{(1+\alpha S)\frac{\mathbf{th}\sqrt{S}}{\sqrt{S}}}{1+\beta S+\gamma S\frac{\mathbf{th}\sqrt{S}}{\sqrt{S}}}$

### 3.6.1 Electrochemical reaction: E-EAR reaction [20]

$$\mathrm{R + s \rightarrow O + s + n_1\ e}$$
$$\mathrm{A^- + s \rightarrow A{,}s + n_2\ e^-}$$

### 3.6.2 Reduced concentration impedance of soluble species R

$$Z(S) = \frac{(1+\alpha S)\,\dfrac{\operatorname{th}\sqrt{S}}{\sqrt{S}}}{1+\beta S+\gamma S\,\dfrac{\operatorname{th}\sqrt{S}}{\sqrt{S}}},\ \alpha,\ \beta,\ \gamma \gtreqless 0 \tag{3.8}$$

### 3.6.3 Nyquist diagrams

Figs. 3.14 and 3.15.

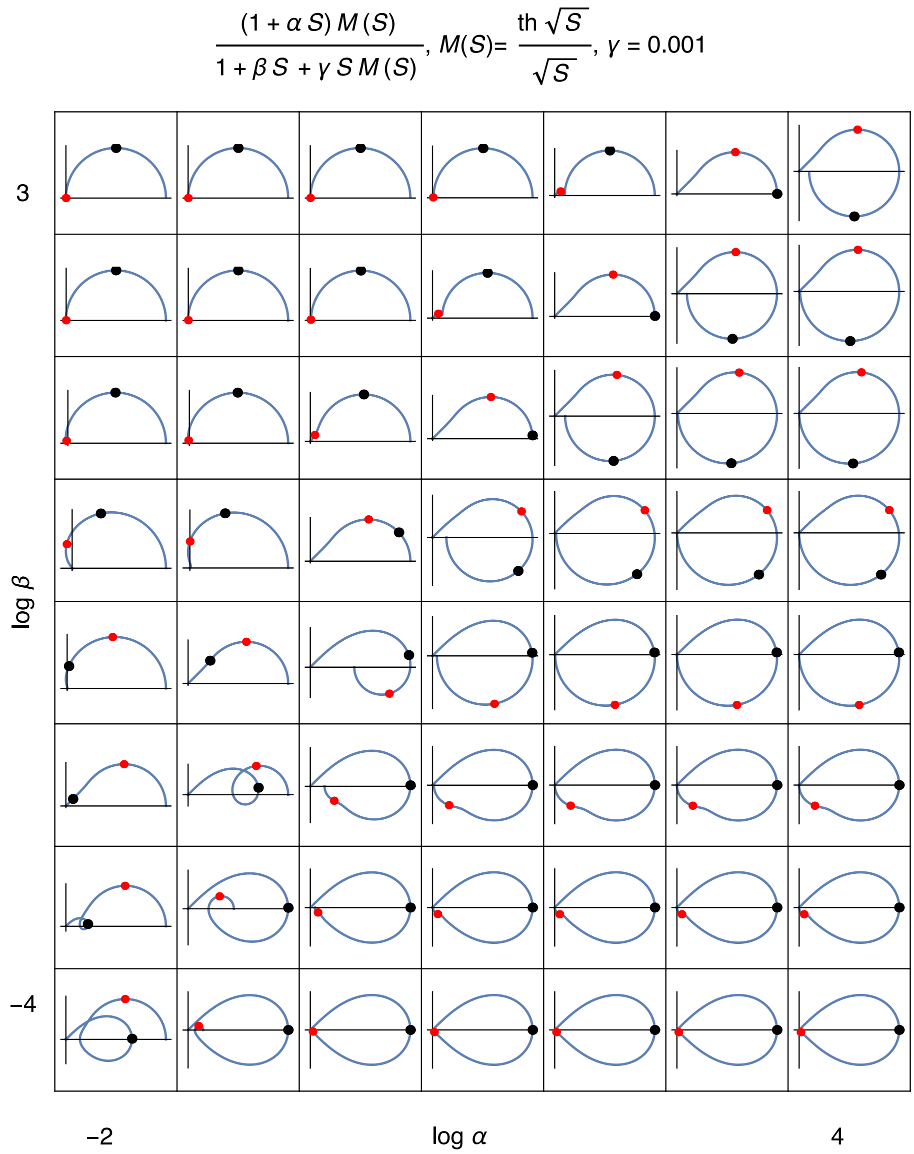


Figure 3.14: Graphics array representation of the Nyquist diagram for the impedance calculated from Eq. (3.8) and plotted using the Nyquist representation (orthonormal scales). Characteristic dimensionless angular frequencies: red dots: $u_{c1} = 2.54$, black dots: $u_{c2} = 1/\beta$. $\gamma = 10^{-3}$.

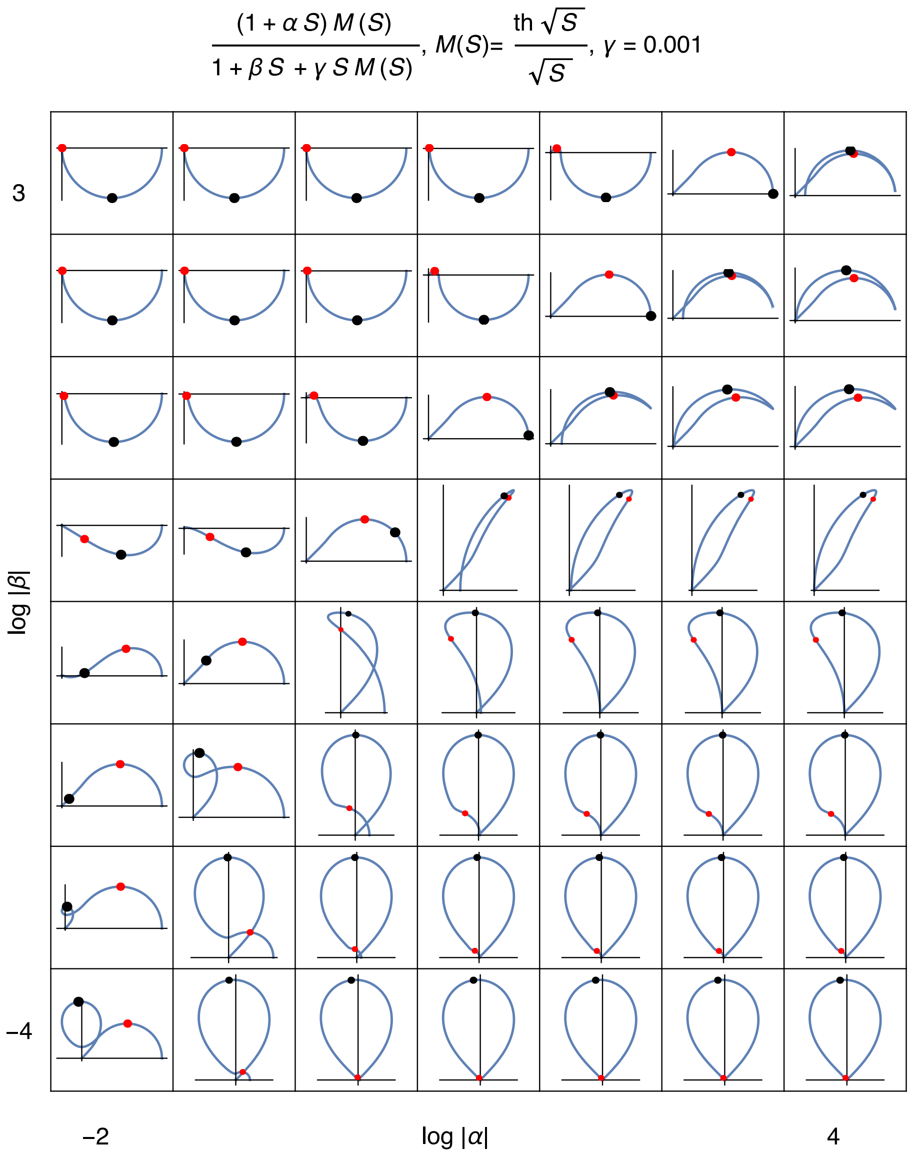


Figure 3.15: Graphics array representation of the Nyquist diagram for the impedance calculated from Eq. (3.8) and plotted using the Nyquist representation (orthonormal scales). $\alpha$, $\beta$, $\gamma < 0$. Characteristic dimensionless angular frequencies: red dots: $u_{c1} = 2.54$, black dots: $u_{c2} = 1/|\beta|$. $\gamma = 10^{-3}$.

# Appendix A

# Some rational fractions in $\sqrt{S}$

## A.1 Introduction

The use of a rational fraction in $\sqrt{S}$

$$Z(\sqrt{S}) = \frac{\sum_{m=0}^{N} b_m (\sqrt{S})^m}{\sum_{p=0}^{P} a_p (\sqrt{S})^p} \tag{A.1}$$

has been proposed by Pintelon et al. [21, 22]. Some rational fraction in $\sqrt{S}$ are studied below.

## A.2 $\dfrac{1}{1+\sqrt{S}}$

$$H(u) = \frac{1}{1+\sqrt{\mathrm{i}\, u}} \tag{A.2}$$

$$\operatorname{Re} H(u) = \frac{\sqrt{2}\sqrt{u}+2}{2\left(u+\sqrt{2}\sqrt{u}+1\right)},\ \operatorname{Im} H(u) = -\frac{\sqrt{u}}{\sqrt{2}\left(u+\sqrt{2}\sqrt{u}+1\right)} \tag{A.3}$$

$$|H(u) - (1/2+\mathrm{i}/2)| = \sqrt{(\operatorname{Re} H(u) - 1/2)^2 + (\operatorname{Im} H(u) - 1/2)^2} = \frac{\sqrt{2}}{2}$$
$$\Rightarrow \text{circle, radius} = \frac{\sqrt{2}}{2} \tag{A.4}$$

Nyquist diagram: Fig. A.1.

## A.3 $\dfrac{1}{1+(\sqrt{S})^3}$

$$H(u) = \frac{1}{1+(\mathrm{i}\, u)^{(3/2)}} \tag{A.5}$$

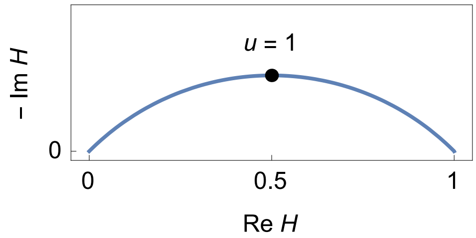


Figure A.1: Nyquist diagram of $\dfrac{1}{1+\sqrt{\mathrm{i}\,u}}$. One quarter circle. $u_c = 1$, $\mathrm{Im}\,H(u_c) = -\dfrac{1}{\sqrt{2}\left(2+\sqrt{2}\right)}$.

$$\mathrm{Re}\,H(u) = \frac{\sqrt{2}u^{3/2}-2}{2\left(\sqrt{2}u^{3/2}-u^3-1\right)},\ \mathrm{Im}\,H(u) = -\frac{u^{3/2}}{-2u^{3/2}+\sqrt{2}u^3+\sqrt{2}} \tag{A.6}$$

$$|H(u)-(1/2-\mathrm{i}/2)| = \sqrt{(\mathrm{Re}\,H(u)-1/2)^2+(\mathrm{Im}\,H(u)-1/2)^2} = \frac{\sqrt{2}}{2}$$
$$\Rightarrow \text{circle, radius} = \frac{\sqrt{2}}{2} \tag{A.7}$$

Remarkable frequencies

$$u_1 = \sqrt[3]{3-2\sqrt{2}},\ u_2 = 1,\ u_3 = \sqrt[3]{2},\ u_4 = \sqrt[3]{3+2\sqrt{2}} \tag{A.8}$$

Nyquist diagram: Fig. A.2.

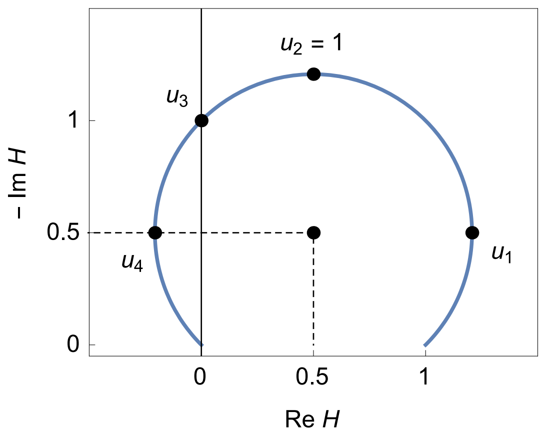


Figure A.2: Nyquist diagram of $\dfrac{1}{1+(\mathrm{i}\,u)^{3/2}}$. Three quarter circle.

## A.4 $\frac{1+(\sqrt{S})^2}{\sqrt{S}\,(1+\alpha(\sqrt{S})^2)}$

$$H(u) = \frac{1+(\sqrt{\mathrm{i}u})^2}{\sqrt{\mathrm{i}u}\,(1+\alpha\,(\sqrt{\mathrm{i}u})^2)} \tag{A.9}$$

$$\mathrm{Re}\ H(u) = \frac{u(\alpha(u-1)+1)+1}{\sqrt{2}\sqrt{u}\,(\alpha^2u^2+1)},\ \mathrm{Im}\ H(u) = \frac{-u(\alpha u+\alpha-1)-1}{\sqrt{2}\sqrt{u}\,(\alpha^2u^2+1)} \tag{A.10}$$

Three different limiting cases

- $\alpha \ll 1$, Nyquist and Bode diagrams: Fig. A.3

$$u_1 = u_{\mathrm{Im}\ H=0} = \frac{-\sqrt{\alpha^2-6\alpha+1}-\alpha+1}{2\alpha} \approx 1 \tag{A.11}$$

$$u_2 = u_{\mathrm{Im}\ H=0} = \frac{+\sqrt{\alpha^2-6\alpha+1}-\alpha+1}{2\alpha} \approx \frac{1}{\alpha} \tag{A.12}$$

- $\alpha = 1$, $H(u) = \frac{1}{\sqrt{\mathrm{i}u}}$

- $\alpha \gg 1$, Nyquist diagram: Fig. A.4

$$u_1 = u_{\mathrm{Re}H=0} = \frac{-\sqrt{\alpha^2-6\alpha+1}+\alpha-1}{2\alpha} \approx \frac{1}{\alpha} \tag{A.13}$$

$$u_2 = u_{\mathrm{Re}H=0} = \frac{\sqrt{\alpha^2-6\alpha+1}+\alpha-1}{2\alpha} \approx 1 \tag{A.14}$$

## A.5 $\frac{1-(\sqrt{S})^2}{\sqrt{S}\,(1-\alpha(\sqrt{S})^2)}$

$$H(u) = \frac{1-(\sqrt{\mathrm{i}u})^2}{\sqrt{\mathrm{i}u}\,(1-\alpha\,(\sqrt{\mathrm{i}u})^2)} \tag{A.15}$$

$$\mathrm{Re}\ H(u) = \frac{u(\alpha+\alpha u-1)+1}{\sqrt{2}\sqrt{u}\,(\alpha^2u^2+1)},\mathrm{Im}\ H(u) = \frac{u(\alpha+\alpha(-u)-1)-1}{\sqrt{2}\sqrt{u}\,(\alpha^2u^2+1)} \tag{A.16}$$

Three different limiting cases

- $\alpha \ll 1$, Nyquist diagram: Fig. A.5

$$u_1 = u_{\mathrm{Re}\ H=0} = \frac{-\sqrt{\alpha^2-6\alpha+1}-\alpha+1}{2\alpha} \approx 1 \tag{A.17}$$

$$u_2 = u_{\mathrm{Re}\ H=0} = \frac{\sqrt{\alpha^2-6\alpha+1}-\alpha+1}{2\alpha} \approx \frac{1}{\alpha} \tag{A.18}$$

- $\alpha = 1$, $H(u) = \frac{1}{\sqrt{\mathrm{i}u}}$

- $\alpha \gg 1$.

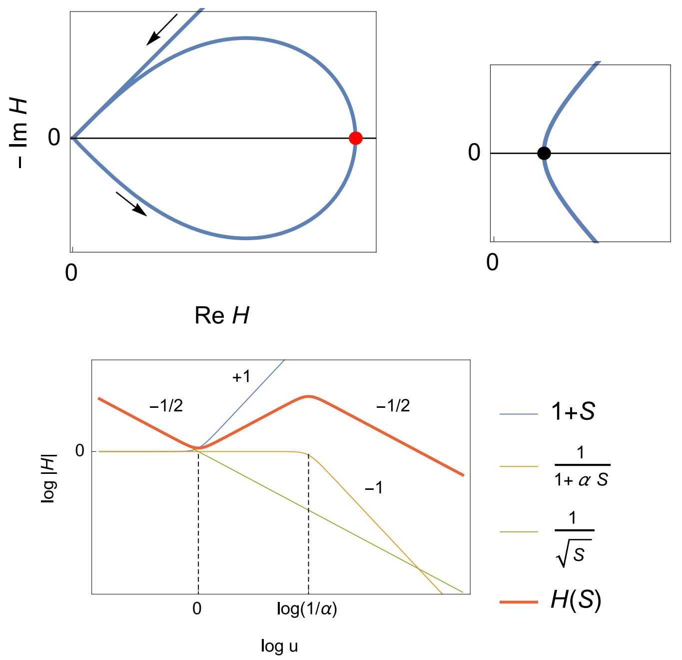


Figure A.3: Nyquist and Bode (modulus) diagram of $\dfrac{1+(\sqrt{\mathrm{i}u})^2}{\sqrt{\mathrm{i}u}\,(1+\alpha\,(\sqrt{\mathrm{i}u})^2)}$. $a \ll 1$. Red dot: $u_2 =\approx 1/\alpha$, black dot: $u_1 = 0 \approx 1$.

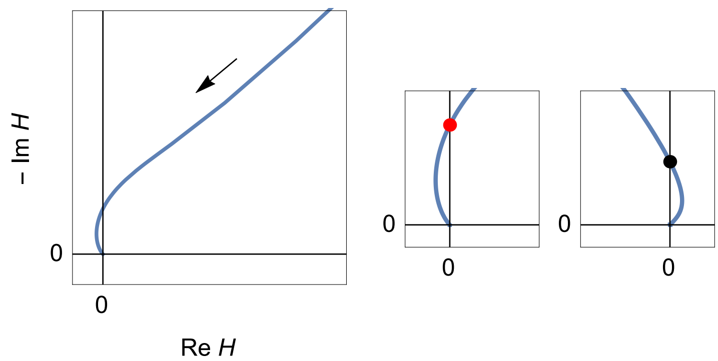


Figure A.4: Nyquist and Bode (modulus) diagram of $\dfrac{1+(\sqrt{\mathrm{i}u})^2}{\sqrt{\mathrm{i}u}\,(1+\alpha\,(\sqrt{\mathrm{i}u})^2)}$. $a \gg 1$. Red dot: $u_{\mathrm{Im\ H=0}} \approx 1/\alpha$, black dot: $u_{\mathrm{Im\ H=0}} \approx 1$.

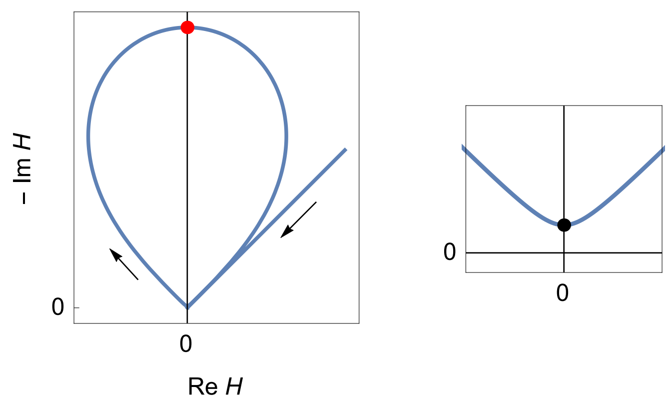


Figure A.5: Nyquist and Bode (modulus) diagram of $\dfrac{1-(\sqrt{\mathrm{i}u})^2}{\sqrt{\mathrm{i}u}\,(1-\alpha\,(\sqrt{\mathrm{i}u})^2)}$. $a \ll 1$. Red dot: $u_2 =\approx 1/\alpha$, black dot: $u_1 = 0 \approx 1$.

# Appendix B

# Impedance structure of reactions involving both adsorbed and soluble species

Table B.1: Impedance structure of reactions involving both adsorbed and soluble species. First order denominator.

| Expression | Reaction | Impedance |
|---|---|---|
| $\dfrac{1+\alpha\,\dfrac{\mathrm{th}\sqrt{S}}{\sqrt{S}}}{1+\beta\,S}$ | (V-H)<br>$A^+ + s + e^- \rightarrow A,s$<br>$A^+ + A,s + e^- \rightarrow A_2 + s$ | $Z_\theta$ |

Table B.2: Impedance structure of reactions involving both adsorbed and soluble species. Second order denominator.

| Expression | Reaction | Impédance |
|---|---|---|
| $\dfrac{1+\alpha\,s+\beta\,\dfrac{\mathrm{th}\sqrt{S}}{\sqrt{S}}+\gamma\,s\,\dfrac{\mathrm{th}\sqrt{S}}{\sqrt{S}}}{1+\delta\,S+\epsilon\,S^2}$ | (V-H) with desorption<br>$A^+ + s + e^- \rightarrow A,s$<br>$A^+ + A,s + e^- \rightarrow A_2,s$<br>$A_2,s \rightarrow A_2 + s$ | $Z_\theta$ |

Table B.3: Impedance structure of reactions involving both adsorbed and soluble species. Dénominateur : $1+\alpha\,S+\beta\,\dfrac{\mathrm{th}\sqrt{S}}{\sqrt{S}}$

| Expressions | Reactions | Impédances |
|---|---|---|
| $\dfrac{1}{1+\alpha\,S+\beta\,\dfrac{\mathrm{th}\sqrt{S}}{\sqrt{S}}}$ | (catalytic)<br>$A^{2+}$ + $B^-$ + s + $e^-$ → AB,s<br>AB,s + $e^-$ → A + $B^-$ + s<br>Hyp. $A^{2+}(0,t) = \mathrm{cte}$ | $Z_\theta$ |
| $\dfrac{\dfrac{\mathrm{th}\sqrt{S}}{\sqrt{S}}}{1+\beta\,s+\gamma\,S\,\dfrac{\mathrm{th}\sqrt{S}}{\sqrt{S}}}$ | (catalytic)<br>$A^{2+}$ + $B^-$ + s + $e^-$ → AB,s<br>AB,s + $e^-$ → A + $B^-$ + s<br>Hyp. $A^{2+}(0,t) = \mathrm{cte}$ | $Z_{\mathrm{B}^-}$ |

Table B.4: Impedance structure of reactions involving both adsorbed and soluble species. Dénominateur : $1+\beta\,S+\gamma\,S\,\dfrac{\mathrm{th}\sqrt{S}}{\sqrt{S}}$.

| Expressions | Reactions | Impedances |
|---|---|---|
| $\dfrac{1+\alpha\,S}{1+\beta\,S+\gamma\,S\,\dfrac{\mathrm{th}\sqrt{S}}{\sqrt{S}}}$ | (V-H)#2<br>$A^+$ + s + $e^-$ → A,s<br>A,s + $e^-$ → $A^-$ + s | $Z_\theta$ |
| $\dfrac{1+\alpha\,\dfrac{\mathrm{th}\sqrt{S}}{\sqrt{S}}}{1+\beta\,S+\gamma\,S\,\dfrac{\mathrm{th}\sqrt{S}}{\sqrt{S}}}$ | (E-EAR)<br>R + s → O + s + $n_1$ e<br>$A^-$ + s ↔ A,s + $n_2$ $e^-$ | $Z_\theta$ |
| $\dfrac{(1+\alpha\,S)\;\dfrac{\mathrm{th}\sqrt{S}}{\sqrt{S}}}{1+\beta\,S+\gamma\,S\,\dfrac{\mathrm{th}\sqrt{S}}{\sqrt{S}}}$ | (E-EAR)<br>R + s → O + s + $n_1$ e<br>$A^-$ + s ↔ A,s + $n_2$ $e^-$ | $Z_\mathrm{R}$ |
| | (V-H)#2<br>$A^+$ + s + $e^-$ → A,s<br>A,s + $e^-$ → $A^-$ + s | $Z_{\mathrm{A}^+}$ |

Table B.5: Impedance structure of reactions involving both adsorbed and soluble species. Dénominateur : $1+\beta\,s+\gamma\,\dfrac{\mathrm{th}\sqrt{S}}{\sqrt{S}}+\delta\,S\,\dfrac{\mathrm{th}\sqrt{S}}{\sqrt{S}}$.

| Expression | Reaction | Impedance |
|---|---|---|
| $\dfrac{1+\alpha\,\dfrac{\mathrm{th}\sqrt{S}}{\sqrt{s}}}{1+\beta\,S+\gamma\,\dfrac{\mathrm{th}\sqrt{S}}{\sqrt{S}}+\delta\,s\,\dfrac{\mathrm{th}\sqrt{S}}{\sqrt{s}}}$ | (DP3)<br>M,s → $M^{2+}$ + s + 2 $e^-$<br>M,s + $A^{2-}$ → MA,s + 2 $e^-$<br>MA,s + B → MAB + s<br>Hyp. $A^{2-}(0,t) = A^{2-*}$ | $Z_\mathrm{s}$ |

# Bibliography


[1] G. C. Temes and J. W. LaPatra. *Introduction to Circuits Synthesis and Design*. McGraw-Hill, New-York, 1977.

[2] R. Curtain and K. Morris. Transfer functions of distributed parameter systems: A tutorial. *Automatica*, 45:1101 – 1116, 2009.

[3] J.-P. Diard, B. Le Gorrec, and C. Montella. *Cinétique électrochimique*. Hermann, Paris, 1996.

[4] Handbook of EIS - Faradaic impedance library. www.bio-logic.info/potentiostat-electrochemistry-ec-lab/apps-literature/eis-literature/hanbook-of-eis/.

[5] Handbook of EIS - Electrical circuits containing CPEs. www.bio-logic.info/potentiostat-electrochemistry-ec-lab/apps-literature/eis-literature/hanbook-of-eis/.

[6] Handbook of EIS - Diffusion impedances. www.bio-logic.info/potentiostat-electrochemistry-ec-lab/apps-literature/eis-literature/hanbook-of-eis/.

[7] J. E. Randles. Kinetics of rapid electrode reactions. *Discuss. Faraday Soc.*, 1:11, 1947.

[8] Interactive equivalent circuit library. http://www.bio-logic.info/potentiostat-electrochemistry-ec-lab/apps-literature/interactive-eis/interactive-faradaic-impedance-library/.

[9] J.-P. Diard and C. Montella. *Impedance of a Redox Reaction (E) at a Rotating Disk Electrode (RDE)*. Wolfram Demonstrations Project, 2010. http://demonstrations.wolfram.com/ImpedanceOfARedoxReactionEAtARotatingDiskElectrodeRDE/.

[10] R. Michel and C. Montella. Diffusion-convection impedance using an efficient analytical approximation of the mass transfer function for a rotating disk. *J. Electroanal. Chem*, 736:139 – 146, 2015.

[11] J.-P. Diard and C. Montella. Re-examination of the diffusion-convection impedance for a uniformly accessible rotating disk. computation and accuracy. *J. Electroanal. Chem.*, 742:37 – 46, 2015.

[12] J. Crank. *The Mathematics of Diffusion*. Clarendon Press, Oxford, 2 edition, 1975.

[13] F. Berthier, J.-P. Diard, B. Le Gorrec, and C. Montella. La résistance de transfert d'électrons d'une réaction électrochimique peut-elle être négative ? *C. R. Acad. Sci. Paris, Série II b*, 325:21–26, 1997.

[14] F. Berthier, J.-P. Diard, and C. Montella. Développement en produits infinis des opérateurs de transport de matière. Application en spectroscopie d'impédance électrochimique et en voltampérométrie linéaire. In C. Gabrielli, editor, *Proceeding*

*of the 11th Forum sur les Impédances Électrochimiques*, pages 189–196, Paris, December 1998.

[15] F. Berthier, J.-P. Diard, and C. Montella. Hopf bifurcation and sign of the transfer resistance. *Electrochim. Acta*, 44:2397–2404, 1999.

[16] F. Berthier, J.-P. Diard, and C. Montella. Numerical solution of coupled systems of ordinary and partial differential equations. Application to the study of electrochemical insertion reaction by linear sweep voltammetry. *J. Electroanal. Chem.*, 502:126–131, 2001.

[17] J.-P. Diard and C. Montella. Non-intuitive features of equivalent circuits for analysis of EIS data. The example of EE reaction. *J. Electroanal. Chem.*, 735:99 – 110, 2014.

[18] C. Gabrielli, P. Moçotéguy, H. Perrot, and R. Wiart. Mechanism of copper deposition in a sulphate bath containing chlorides. *J. Electroanal. Chem.*, 572:367–375, 2004.

[19] J.-P. Diard and C. Montella. Unusual concentration impedance for catalytic copper deposition. *J. Electroanal. Chem.*, 590:126–137, 2006.

[20] M.B. Molina Concha, M. Chatenet, C. Montella, and J.-P. Diard. A Faradaic impedance study of E-EAR reaction. *J. Electroanal. Chem*, 696:24 – 37, 2013.

[21] R. Pintelon and J. Schoukens. *System Identification. A frequency domain approach*. IEEE Press, Piscataway, USA, 2001.

[22] L. Pauwels, W. Simons, A. Hubin, J. Schoukens, and R. Pintelon. Key issues for reproducible impedance measurements and their well-founded error analysis in a silver electrodeposition system. *Electrochim. Acta*, 47:2135 – 2141, 2002.